

Effective Gradient Sample Size via Variation Estimation for Accelerating Sharpness aware Minimization

Jiixin Deng¹, Junbiao Pang¹, Baochang Zhang², Tian Wang²

¹Beijing University of Technology

²Beihang University

dengjiixin@emails.bjut.edu.cn, junbiao_pang@bjut.edu.cn, bczhang@buaa.edu.cn, wangtian@buaa.edu.cn

Abstract

Sharpness-aware Minimization (SAM) has been proposed recently to improve model generalization ability. However, SAM calculates the gradient twice in each optimization step, thereby doubling the computation costs compared to stochastic gradient descent (SGD). In this paper, we propose a simple yet efficient sampling method to significantly accelerate SAM. Concretely, we discover that the gradient of SAM is a combination of the gradient of SGD and the Projection of the Second-order gradient matrix onto the First-order gradient (PSF). PSF exhibits a gradually increasing frequency of change during the training process. To leverage this observation, we propose an adaptive sampling method based on the variation of PSF, and we reuse the sampled PSF for non-sampling iterations. Extensive empirical results illustrate that the proposed method achieved state-of-the-art accuracies comparable to SAM on diverse network architectures.

1 Introduction

The powerful generalization ability of Deep Neural Networks (DNNs) has led to significant success in many fields [Chaudhari *et al.*, 2019; Izmailov *et al.*, ; Kwon *et al.*, 2021]. In recent years, some research has been proposed to understand the generalization of DNNs [Keskar *et al.*, 2017; Zhang *et al.*, 2021; Mulayoff and Michaeli, 2020; Andriushchenko and Flammarion, 2022; Zhou *et al.*, 2021; Zhou *et al.*, 2022]. Several studies have verified the relationship between flat minima and generalization error [Dinh *et al.*, 2017; Li *et al.*, 2018; Jiang *et al.*, 2020; Liu *et al.*, 2020; Sun *et al.*, 2021]. Among these studies, Jiang *et al.* [Jiang *et al.*, 2020] explored over 40 complexity measures and demonstrated that a sharpness-based measure exhibits the highest correlation with generalization.

Based on the connection between sharpness of the loss landscape and model generalization, Foret *et al.* proposes Sharpness Aware Minimization (SAM) [Foret *et al.*, 2021] to seek out parameter values whose entire neighborhoods have uniformly low training loss value. SAM minimizes both

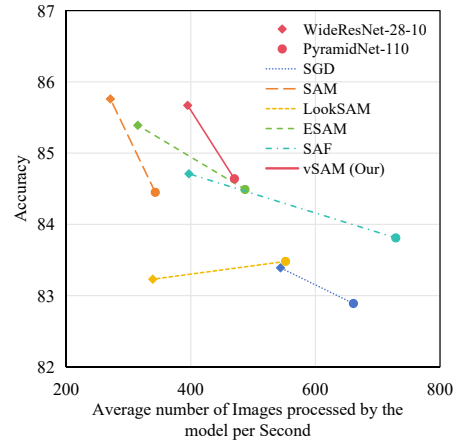


Figure 1: Accuracy vs training speed of SGD, SAM, LookSAM, ESAM, SAF and vSAM (Our). Every connected line represents a method that trains WideResNet-28-10 and PyramidNet-110 models on CIFAR-100. vSAM substantially accelerates training with almost no reduction in accuracy.

the loss value and the loss sharpness to obtain a flat minimum and improve model generalization. SAM and its variants have demonstrated state-of-the-art performance across various applications [Kwon *et al.*, 2021; Du *et al.*, 2022a; Liu *et al.*, 2022; Chen *et al.*, 2022; Zheng *et al.*, 2021; Zhuang *et al.*, 2022]. However, SAM requires two forward and backward operations in one iteration, which results in SAM’s optimization speed being only half that of SGD. In some scenarios, dedicating twice the training time to achieve only a marginal improvement in accuracy may not strike an optimal balance between accuracy and efficiency. For example, when SAM is employed to optimize WideResNet-28-10 on CIFAR-100, despite achieving a higher test accuracy than SGD (84.45% vs. 82.89%), the optimization speed is only half that of SGD (343 imgs/s vs. 661 imgs/s), as illustrated in Figure 1.

In this paper, we accelerate SAM by introducing an adaptive gradient sampling strategy, ensuring nearly no drop in accuracy. Specifically, we have observed that the gradient of SAM can be decomposed into two parts: the first part is the gradient of SGD, which searches for a local minimum, while the second part is the Projection of the Second-order gradi-

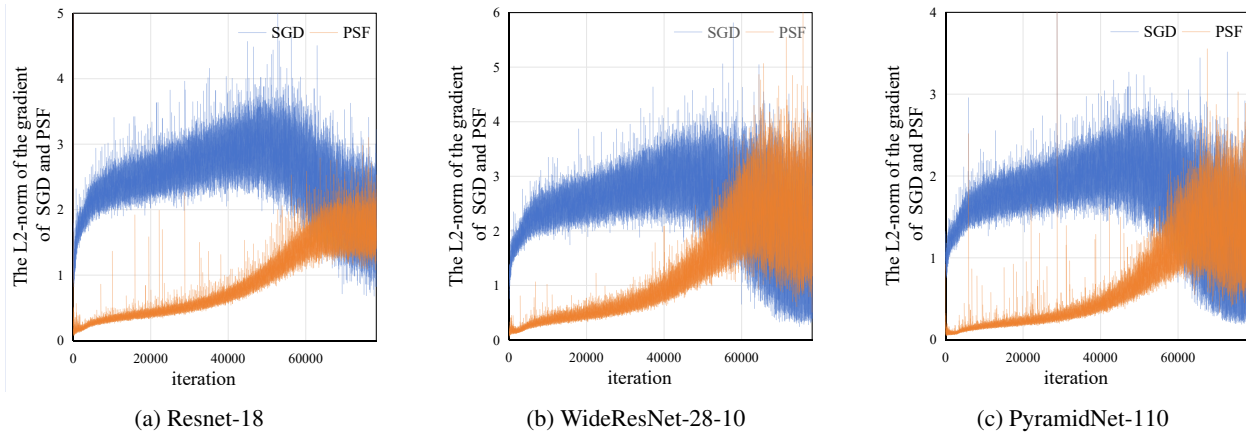


Figure 2: The variation trend of $\|\nabla L_i^{SGD}\|$ and $\|\nabla L_i^{PSF}\|$ during training. $\|\nabla L_i^{SGD}\|$ and $\|\nabla L_i^{PSF}\|$ are denotes the L2-norm of the gradient of SGD and the L2-norm of PSF, respectively. The trends of $\|\nabla L_i^{SGD}\|$ and $\|\nabla L_i^{PSF}\|$ are similar across different models (Resnet-18, WideResNet-28-10, PyramidNet-110).

ent matrix onto the First-order gradient (PSF), which drives SAM to search for a flat region. As illustrated in Fig. 2, the L2-norm of PSF (hereinafter referred to as L2-PSF) gradually increases with iterations, and its amplitude changes from small values to large ones. This indicates that the efficacy of the PSF varies throughout the training process. Motivated by the observation in Fig. 2, we propose to accelerate SAM by adaptively sampling the PSF. Concretely, during the sampling iterations, we compute the PSF, while during the non-sampling iterations, we reuse the previously computed PSF. By controlling the sampling rate, we can significantly speed up the optimization process by reducing the computation of the PSF.

In this paper, we propose Variation-based SAM (vSAM) to adaptively adjust the sampling rate based on the variance of the L2-PSF. The variance is a natural way to measure the sampling ratio, reflecting the difference of the PSF between two iterations. We increase the sampling rate of the PSF to ensure that the model’s generalization ability does not degrade when the PSF changes significantly, while we reduce the sampling rate of the PSF when the gradient of SGD dominates the optimization. In this way, we speed up the optimization while maintaining the generalization performance of the model.

In a nutshell, our contributions are as follows:

- To the best of our knowledge, we firstly find that the gradient of SAM can be decomposed into the gradient of SGD and PSF. Furthermore, we observe a gradual increase in the L2-norm of PSF across various networks during training, with its amplitude changing from small to large values. This observation motivates us to adaptively sample the PSF to accelerate SAM.
- We introduce the vSAM, which adaptively samples and reuses gradients to not only preserve the model’s generalization ability but also accelerate the optimization efficiency. The empirical results demonstrate that vSAM achieves a 40% acceleration compared to SAM, while ensuring almost no decrease in model generalization ability.

2 Related Works

Background of SAM. The notion of seeking minima that are "flat minima" can be credited to [Hochreiter and Schmidhuber, 1994], and there has been considerable research examining its relationship with generalization [Zhang *et al.*, 2021; Keskar *et al.*, 2017; Wei and Ma, 2019; Jiang *et al.*, 2020]. Based on these studies, Foret *et al.* [Foret *et al.*, 2021] introduced an effective approach to improving the model’s generalization ability, called SAM. The optimization process of SAM can be viewed as addressing a minimax optimization problem, formulated as follows:

$$\min_{\mathbf{w}} L^{SAM}(\mathbf{w}) + \lambda \|\mathbf{w}\|_2^2 \quad (1)$$

$$\text{where } L^{SAM}(\mathbf{w}) = \max_{\|\boldsymbol{\varepsilon}\| \leq \rho} L(\mathbf{w} + \boldsymbol{\varepsilon}),$$

where $\boldsymbol{\varepsilon}$ represents weight perturbations in Euclidean ball with radius ρ , L^{SAM} is the perturbed loss, $\lambda \|\mathbf{w}\|_2^2$ is a standard L2 regularization term. In order to minimize $L^{SAM}(\mathbf{w})$, SAM utilizes Taylor expansion to search for the maximum perturbed loss in local parameter space:

$$\arg \max_{\|\boldsymbol{\varepsilon}\| \leq \rho} L(\mathbf{w} + \boldsymbol{\varepsilon}) \approx \arg \max_{\|\boldsymbol{\varepsilon}\| \leq \rho} L(\mathbf{w}) + \boldsymbol{\varepsilon}^T \nabla_{\mathbf{w}} L(\mathbf{w}) \quad (2)$$

$$= \arg \max_{\|\boldsymbol{\varepsilon}\| \leq \rho} \boldsymbol{\varepsilon}^T \nabla_{\mathbf{w}} L(\mathbf{w}),$$

By solving Eq. (2), SAM can calculate the gradient once to obtain the perturbation $\hat{\boldsymbol{\varepsilon}} = \rho \nabla_{\mathbf{w}} L(\mathbf{w}) / \|\nabla_{\mathbf{w}} L(\mathbf{w})\|$ that can maximize the loss function. Minimizing the loss of the perturbed weight $\mathbf{w} + \hat{\boldsymbol{\varepsilon}}$ promotes the entire neighborhood of the weight \mathbf{w} to have low training loss values. Through gradient approximation, the optimization problem of SAM is reduced to:

$$\min_{\mathbf{w}} L^{SAM}(\mathbf{w}) \approx \min_{\mathbf{w}} L(\mathbf{w} + \hat{\boldsymbol{\varepsilon}}), \quad (3)$$

Finally, SAM requires a second calculation of the gradient to optimize the model, as follows:

$$\nabla_{\mathbf{w}} L^{SAM}(\mathbf{w}) \approx \nabla_{\mathbf{w}} L(\mathbf{w} + \hat{\boldsymbol{\varepsilon}}) \approx \nabla_{\mathbf{w}} L(\mathbf{w})|_{\mathbf{w} + \hat{\boldsymbol{\varepsilon}}}, \quad (4)$$

From Eq. (2) and Eq. (4), we observe that SAM necessitates two forward and backward operations to update weights once. **Efficient optimization methods for SAM.** Some methods have been proposed to enhance the optimization speed of SAM, broadly categorized into two groups.

The first category of methods focuses on reducing the data and model weights involved in training. For example, Du et al. propose ESAM [Du et al., 2022a], which employs two training strategies, Stochastic Weight Perturbation (SWP) and Sharpness Sensitive Data Selection (SDS), to reduce computation. SWP approximates the weight perturbation by using a subset of model weights, while SDS updates the model using a subset of training data that contributes the most to sharpness. However, SWP barely accelerates training speed since that gradients should be computed for almost every weight, while SDS still requires a forward and backward in each optimization step.

The second category of methods focuses on reducing the computation of gradients. For example, Du et al. propose SAF and MESA [Du et al., 2022b], which employ trajectory loss to approximate sharpness through a surrogate sharpness measure (the loss of SGD between several iterations). SAF and MESA lacks direct weight perturbations to assist SAM in escaping local minimum regions (as discussed in Experiments section). Additionally, SAF requires a large amount of memory to store the output results for all data, while MESA also needs to maintain an Exponential Moving Average (EMA) model during training. Liu et al. propose Look-SAM [Liu et al., 2022] which periodically calculates the gradient of SAM every 5 iterations. This periodic strategy ensures that the majority of optimization steps do not require two forward and backward passes. However, this uniform gradient sampling fails to reflect the importance of sharpness optimization in the overall optimization process. Subsequently, Jiang et al. claims that the SAM update is more useful in sharp regions than in flat regions. As a result, they design AE-SAM [Jiang et al., 2023] to adaptively employ SAM based on the loss landscape geometry. However, it requires sharpness to be evaluated at each optimization step. In this paper, we propose an adaptive sampling strategy to reflect the importance of sharpness and adjust the sampling rate of the PSF.

3 Method

3.1 Gradient Composition of SAM

We rewrite Eq. (4) based on Taylor expansion and substitute $\hat{\varepsilon}$ to obtain the following:

$$\begin{aligned} \nabla_{\mathbf{w}}L(\mathbf{w} + \hat{\varepsilon}) &\approx \nabla_{\mathbf{w}}(L(\mathbf{w}) + \hat{\varepsilon}\nabla_{\mathbf{w}}L(\mathbf{w})) \\ &= \nabla_{\mathbf{w}}(L(\mathbf{w}) + \rho\|\nabla_{\mathbf{w}}L(\mathbf{w})\|). \end{aligned} \quad (5)$$

The gradient of SAM can be considered as a combination of SGD’s gradient and the gradient of the L2-norm of SGD’s gradient. We expand the second term in Eq. (5) as follows:

$$\nabla_{\mathbf{w}}(\rho\|\nabla_{\mathbf{w}}L(\mathbf{w})\|) = \rho \frac{\nabla_{\mathbf{w}}L(\mathbf{w})\nabla_{\mathbf{w}}^2L(\mathbf{w})}{\|\nabla_{\mathbf{w}}L(\mathbf{w})\|}. \quad (6)$$

The L2-norm of SGD’s gradient (hereinafter referred to as L2-SGD) can be transformed into the Projection of the

Second-order gradient matrix onto the First-order gradient (PSF). Eq. (5) and Eq. (6) indicate that the gradient of SAM can be decomposed into the gradient of SGD and PSF. The PSF prompts SAM to find a flat minimum.

Lemma 1. Let $\nabla_{\mathbf{w}}^2L(\mathbf{w})$ be a positive definite matrix with n eigenvalues, then the L2-PSF has an upper bound as follows:

$$\|\nabla_{\mathbf{w}}(\rho\|\nabla_{\mathbf{w}}L(\mathbf{w})\|)\| \leq \rho \sum_{i=1}^n \delta_i |\cos(\theta_i)|, \quad (7)$$

where δ_i is the i -th eigenvalue, θ_i is the angle between U_i and $\nabla_{\mathbf{w}}L(\mathbf{w})$, U_i is the i -th eigenvector of $\nabla_{\mathbf{w}}^2L(\mathbf{w})$.

We observe that the L2-PSF gradually increases during training, and its amplitude changes from small values to large ones, as shown in Figure 2. From Lemma 1, we can see that the L2-PSF is related to the eigenvalues of matrix $\nabla_{\mathbf{w}}^2L(\mathbf{w})$, as well as the angle formed between the eigenvectors and the gradient $\nabla_{\mathbf{w}}L(\mathbf{w})$. The changes in the L2-PSF may be attributed to more pronounced variations in the direction of $\nabla_{\mathbf{w}}L(\mathbf{w})$ during the later stages of optimization. The observed phenomenon reflects the evolving significance of the PSF during the training process, prompting us to utilize the variance of the L2-PSF (i.e., $\|\nabla L_i^{PSF}\| = \|\nabla L_i^{SAM} - \nabla L_i^{SGD}\|$) for effective control of gradient sampling during training. We adjust the sampling rate according to the following rules:

- When the PSF changes slowly, the PSF in the current iteration can be replaced by the PSF in the previous iteration. We decrease the sampling rate to alleviate the computational burden of the PSF.
- When the PSF changes rapidly, we enhance the sampling rate to calculate the PSF in a high frequency. This ensures that the gradient is similar to the original SAM, thereby improving the generalization ability of the model.

3.2 Effective Gradient Sample Size via Variation Estimation

Adaptive gradient sampling based on variance. In order to estimate the variance of $\|\nabla L^{PSF}\|$, we save $\|\nabla L^{PSF}\|$ in the previous N sampled iterations and denote as \mathbf{g}^{norm} . However, there might be individual values in \mathbf{g}^{norm} that are extremely large or small, as shown in Figure 2. Using the overall variance of these L2-norm values directly could impact the variation of the sampling rate. Therefore, we propose sort \mathbf{g}^{norm} in ascending order and denote the result as $\hat{\mathbf{g}}^{norm}$. The sorted values are then evenly divided into M slices and denoted as $[\hat{\mathbf{g}}_1^{norm}, \dots, \hat{\mathbf{g}}_M^{norm}]$. Finally, we calculate the variance of L2-norm values within each slice and compute the average of these variances as follows:

$$v_i = \frac{1}{M} \sum_{j=1}^M var(\hat{\mathbf{g}}_j^{norm}), \quad (8)$$

where $var(\mathbf{g})$ is a function for calculating the variance of \mathbf{g} , v_i evaluates the variance of the PSF in the i -th iteration. The change rate of the variance at i -th iteration can be written as follows:

$$c_i^{var} = \frac{v_i - v_{i-1}}{v_{i-1}}. \quad (9)$$

To more accurately evaluate changes in variance of the previous N sampled iterations, we calculate the change rate according to Eq. (9) at each sampled iteration and average it as follows:

$$\hat{c}^{var} = \frac{1}{N-1} \sum_{i=2}^N c_i^{var}. \quad (10)$$

Adaptive gradient sampling based on norm value. When the gradient of SGD dominates the training, we aim to speed up the optimization by reducing the computation of the PSF. We use the ratio of $\|\nabla L_i^{PSF}\|$ to $\|\nabla L_i^{SGD}\|$ at the i -th iteration as a factor controlling the sampling rate, as follows:

$$r_i = \frac{\|\nabla L_i^{PSF}\|}{\|\nabla L_i^{SGD}\|}. \quad (11)$$

In Eq. (11), r_i reflects the relative importance between PSF and SGD during the optimization process. The change rate of the ratio at the i -th iteration and average change rate in the previous N sampled iterations can be written as Eq. (12) and Eq. (13), respectively.

$$c_i^{norm} = \frac{r_i - r_{i-1}}{r_{i-1}}, \quad (12)$$

$$\hat{c}^{norm} = \frac{1}{N-1} \sum_{i=2}^N c_i^{norm}. \quad (13)$$

We adjust the sampling rate in an autoregressive manner, the sampling rate for the next N iterations be written as follows:

$$s_{i+1} = s_i \cdot (1 + \alpha \cdot \hat{c}^{var} + \alpha \cdot \hat{c}^{norm}), \quad (14)$$

$$p_{i+1} = \frac{s_{i+1}}{N}, \quad (15)$$

where s_i is the number of sampling required in the last N iterations, α is a hyperparameter that can adjust the variation of the sampling rate, and p_{i+1} is the sampling rate in the next N iterations. In the next N iterations, the PSF is sampled with a probability of p_{i+1} in each iteration. In Eq. (14), we can see that the number of samples required for the next N iterations will be controlled by \hat{c}^{var} and \hat{c}^{norm} . In addition, the computational cost of L2-norm becomes larger as the model size increases. We observe that the L2-SGD and the L2-PSF in the last few layers of the model also capture the changes in the gradient of SGD and PSF. Thus, we replace $\|\nabla L^{SGD}\|$ and $\|\nabla L^{PSF}\|$ with the L2-SGD and the L2-PSF in the last few layers of the model, respectively.

Gradient reuse in the non-sampling iteration. In the sampling iteration, the optimization rule can be written as follows:

$$\mathbf{w}_{i+1} = \mathbf{w}_i - \eta \nabla L_i^{SAM} \quad (16)$$

where η is learning rate. Eq. (16) is essentially the optimization rule for SAM. In the non-sampling iteration, we reuse the PSF from the last sampling iteration, and the optimization rule can be written as follows:

$$\mathbf{w}_{i+1} = \mathbf{w}_i - \eta (\nabla L_i^{SGD} + \gamma^{i-i^*} \cdot \nabla L_{i^*}^{PSF}) \quad (17)$$

where i^* represents the last sampling in the i^* -th iteration, $\nabla L_{i^*}^{PSF}$ is the PSF at the last sampling iteration, and γ is a

Algorithm 1 Pseudocode of the proposed vSAM

Require: The training dataset, the learning rate η , parameters $\alpha, \gamma, \rho, N, M$.

- 1: Initialization: s_1 , iteration I_{start} to start applying the adaptive sampling rate.
 - 2: **for** $i = 1, 2, \dots$ **do**
 - 3: Calculating the gradient of SGD ∇L_i^{SGD} ;
 - 4: **if** $i \leq I_{start}$ **or** sampling **then**
 - 5: Calculating the gradient of SAM ∇L_i^{SAM} ;
 - 6: Calculating the PSF ∇L_i^{PSF} ;
 - 7: $\mathbf{w}_{i+1} = \mathbf{w}_i - \eta \nabla L_i^{SAM}$;
 - 8: **else**
 - 9: $\mathbf{w}_{i+1} = \mathbf{w}_i - \eta (\nabla L_i^{SGD} + \gamma^{i-i^*} \cdot \nabla L_{i^*}^{PSF})$;
 - 10: **end if**
 - 11: **if** $i > I_{start}$ **and** $i \% N == 0$ **then**
 - 12: compute sampling rate p ;
 - 13: **end if**
 - 14: **end for**
-

hyperparameter that reduces the magnitude of the PSF. The reliability of the PSF obtained from the last sampling diminishes progressively as the current iteration distances itself from the last sampled iteration. Algorithm 1 shows the overall proposed algorithm.

Convergence analysis. We further analyze the convergence properties of vSAM as follows.

Lemma 2. *Suppose $L^{SGD}(\mathbf{w})$ is τ -Lipschitz smooth and $|L^{SGD}(\mathbf{w})|$ is bounded by M . For any $t \in \{0, \dots, T\}$ and any $\mathbf{w} \in W$, suppose we can obtain bounded observations as follows:*

$$\begin{aligned} \mathbb{E}[\nabla L_t^{SGD}(\mathbf{w})] &= \nabla L^{SGD}(\mathbf{w}), \|\nabla L_t^{SGD}(\mathbf{w})\| \leq G_1, \\ \mathbb{E}[\nabla L_t^{PSF}(\mathbf{w})] &= \nabla L^{PSF}(\mathbf{w}), \|\nabla L_t^{PSF}(\mathbf{w})\| \leq G_2. \end{aligned} \quad (18)$$

Then with learning rate $\eta_t = \frac{\eta_0}{t}$, we have the following bound for vSAM:

$$\begin{aligned} \frac{1}{T} \sum_{t=1}^T \mathbb{E}[\|\nabla L^{SGD}(\mathbf{w}) + \gamma \nabla L^{PSF}(\mathbf{w})\|^2] \\ \leq C_1 + C_2 \ln T \end{aligned} \quad (19)$$

where C_1 and C_2 are constants that only depend on $\tau, \gamma, \eta_0, M, G_1$ and G_2 .

It can be seen from Lemma 2 that the convergence of vSAM is affected by the parameter γ , the learning rate η_0 , etc., while they are all controlled within a certain range.

4 Experimental Results

4.1 Setup

Datasets. To verify the effectiveness of vSAM, we conduct experiments on CIFAR-10 and CIFAR-100 [Krizhevsky *et al.*, 2009] image classification benchmark datasets.

Models. We employ a variety of architectures, i.e. ResNet-18 [He *et al.*, 2016], WideResNet-28-10 [Zagoruyko and Komodakis, 2016] and PyramidNet-110 [Han *et al.*, 2017] to evaluate the performance and training efficiency.

α	Accuracy	Sampling number	AIS
SAM	84.45	78200	343(100%)
0.05	83.25	5224	596(174%)
0.1	84.01	15287	461(134%)
0.13	84.52	26466	484(141%)
0.15	84.28	39276	406(118%)
0.2	84.66	35150	444(129%)

Table 1: Parameter Study of α on CIFAR-100 datasets with WideResNet. The best accuracy and efficiency are bolded.

Baselines. We take the vanilla SGD and SAM [Foret *et al.*, 2021] as baselines. To comprehensively evaluate the performance of vSAM, we have also chosen some efficient methods SAM-5, SAM-10, ESAM [Du *et al.*, 2022a], and LookSAM [Liu *et al.*, 2022], SAF [Du *et al.*, 2022b], MESA [Du *et al.*, 2022b] and AE-SAM [Jiang *et al.*, 2023] for comparison. SAM-5 and SAM-10 indicate that SAM is used every 5 and 10 iterations respectively, while SGD is used for other iterations. Other efficient methods are the follow-up works of SAM that aim to enhance efficiency. We re-implemented the SAM, SAM-5, SAM-10, LookSAM, ESAM and SAF in Pytorch.

Implementation details. On CIFAR-10 and CIFAR-100, we train all the models 200 epochs using a batch size of 128 with cutout regularization [DeVries and Taylor, 2017] and cosine learning rate decay [Loshchilov and Hutter, 2016]. For the proposed method, we set $\gamma = 0.7$ for ResNet-18, $\gamma = 0.9$ for WideResNet-28-10 and PyramidNet-110, and use $K = 50$, $M = 5$ for all experiments. For other hyperparameters, we follow the setup in ESAM. We implement vSAM in Pytorch and train models on a single NVIDIA GeForce RTX 3090 three times, each with different random seed. The adaptive gradient sampling will be deployed after a predefined iteration I_{start} , because the variance and norm value of the PSF are neither stable nor reliable at the first few epochs.

Additionally, to avoid using the PSF in every iteration, we set the maximum sampling rate to 0.8 and halt sampling when the sampling number reaches $0.8 \times N$ within the current N iterations.

The number of images processed per second may change during training. Therefore, optimization efficiency is evaluated by calculating costs and quantified by the Average number of Images processed by the model per Second (AIS) as follows:

$$AIS = \frac{D \cdot E}{T}, \quad (20)$$

where D represents the amount of data for one epoch of training, T is the total training time in seconds, including both data loading and model optimization time, and E represents the training epoch.

4.2 Parameter Studies

Parameter study of α . We study the effect of α on accuracy and optimization efficiency using the WideResNet-28-10 model on the CIFAR-100 dataset. The results are presented in Table 1. As α increases gradually, we observe a correspond-

γ	Accuracy	Sampling number	AIS
0.6	83.93	21219	508
0.7	84.52	26372	486
0.8	84.52	26466	484
0.9	84.64	28288	469

Table 2: Parameter Study of γ on CIFAR-100 datasets with WideResNet. The best accuracy and efficiency are bolded.

ing increase in the sampling number, leading to a slowdown in training speed. However, the accuracy is improved with the sampling number increases.

Moreover, the maximum sampling number does not mean the best accuracy. It indicates that sampling at the opportune moments is more crucial than sampling number. For example, vSAM shows a significant improvement in optimization speed compared to SAM and achieves better accuracy than SAM-5 with nearly identical sampling number. Across all our experiments, we set $\alpha = 0.1$ for CIFAR-10 and $\alpha = 0.13$ for CIFAR-100 to ensure that vSAM improves the optimization speed by about 40% compared to SAM

Parameter study of γ . We study the effect of γ on accuracy and optimization efficiency using the WideResNet-28-10 model on the CIFAR-100 dataset. The results are presented in Table 2. We observe that γ has a small effect on optimization speed, and gradient reuse plays a limited role when γ is small. Therefore, we recommend using a large value for γ in most of cases.

4.3 Comparison to SOTAs

We perform experiments to train ResNet-18, WideResNet-28-10, and PyramidNet-110 on CIFAR-10 and CIFAR-100. The experimental results are presented in Table 3. We evaluate the proposed method and comparative methods from two aspects: classification accuracy and optimization efficiency.

Accuracy. From Table 3, we observe that vSAM achieves significantly higher accuracy compared to SGD, SAM-5, and SAM-10. The accuracy of vSAM is comparable to or even surpasses that of SAM. Furthermore, in comparison to LookSAM, ESAM, and AE-SAM, our results outperform theirs in most cases. This demonstrates that vSAM can successfully preserve the model’s generalization ability during the training process. Because vSAM calculates the PSF in more appropriate optimization iterations, it promotes generalization. vSAM reuses the PSF term in the non-sampling iteration also guarantees the generalization ability of the model. We also achieve superior results compared to SAF and MESA. Because SAF and MESA optimize the sharpness from multiple previous iteration to the current iteration, which is different from the sharpness of the current iteration. SAF would overlook the local sharpness because multiple local sharpness tends to occur the multiple optimization iterations [Zhang *et al.*, 2023].

Efficiency. These experiments demonstrate that vSAM exhibits about 40% faster training than SAM while achieving comparable accuracy. While SAM-5 and SAM-10 enhance optimization speed, they exhibit a significant decrease in accuracy. In certain scenarios, vSAM exhibits a faster op-

	CIFAR-10			CIFAR-100		
ResNet	Accuracy \uparrow	Sampling number \downarrow	AIS \uparrow	Accuracy \uparrow	Sampling number \downarrow	AIS \uparrow
SGD	96.13 \pm 0.03	\	3167(178%)	79.22 \pm 0.12	\	3194(174%)
SAM	96.62 \pm 0.04	78200	1780(100%)	<u>80.66\pm0.06</u>	78200	1836(100%)
SAM-5	96.40 \pm 0.04	15640	2780(156%)	80.42 \pm 0.09	15640	2763(151%)
SAM-10	96.28 \pm 0.05	7820	2982(168%)	80.27 \pm 0.06	7820	2969(162%)
LookSAM-5	96.33 \pm 0.04	15640	2106(118%)	80.21 \pm 0.05	15640	2186(119%)
ESAM	96.55 \pm 0.03	\	1895(107%)	80.01 \pm 0.12	\	1919(105%)
ESAM ¹	96.56 \pm 0.08	\	2409(140%)	80.41 \pm 0.10	\	2423(140%)
SAF	96.26 \pm 0.02	\	2696(152%)	79.93 \pm 0.04	\	2686(146%)
SAF ²	96.37 \pm 0.02	\	3213(194%)	80.06 \pm 0.05	\	3248(192%)
MESA ²	96.24 \pm 0.02	\	2780(168%)	79.79 \pm 0.09	\	2793(165%)
AE-SAM ³	<u>96.63\pm0.04</u>	39178	\	80.48 \pm 0.11	38944	\
vSAM	96.64\pm0.12	23579	2492(140%)	80.76\pm0.15	27377	2470(135%)
WideResNet	Accuracy \uparrow	Sampling number \downarrow	AIS \uparrow	Accuracy \uparrow	Sampling number \downarrow	AIS \uparrow
SGD	96.89 \pm 0.02	\	666(197%)	82.89 \pm 0.06	\	661(193%)
SAM	<u>97.43\pm0.04</u>	78200	338(100%)	84.45 \pm 0.05	78200	343(100%)
SAM-5	97.16 \pm 0.03	15640	553(164%)	83.06 \pm 0.08	15640	549(160%)
SAM-10	96.94 \pm 0.02	7820	605(179%)	83.07 \pm 0.08	7820	608(177%)
LookSAM-5	97.05 \pm 0.03	15640	537(159%)	83.48 \pm 0.06	15640	552(161%)
ESAM	97.44\pm0.03	\	480(142%)	84.49 \pm 0.05	\	487(142%)
ESAM ¹	97.29 \pm 0.11	\	550(139%)	84.51 \pm 0.01	\	545(139%)
SAF	97.08 \pm 0.04	\	628(186%)	82.33 \pm 0.03	\	633(185%)
SAF ²	97.08 \pm 0.15	\	727(198%)	83.81 \pm 0.04	\	729(197%)
MESA ²	97.16 \pm 0.23	\	617(168%)	83.59 \pm 0.24	\	625(169%)
AE-SAM ³	97.30 \pm 0.10	38709	\	<u>84.51\pm0.11</u>	38787	\
vSAM	97.29 \pm 0.08	33251	468(139%)	84.64\pm0.17	29356	470(137%)
PyramidNet	Accuracy \uparrow	Sampling number \downarrow	AIS \uparrow	Accuracy \uparrow	Sampling number \downarrow	AIS \uparrow
SGD	97.04 \pm 0.03	\	544(200%)	83.39 \pm 0.04	\	544(201%)
SAM	97.72 \pm 0.02	78200	272(100%)	85.76\pm0.06	78200	271(100%)
SAM-5	97.57 \pm 0.05	15640	447(164%)	84.25 \pm 0.05	15640	457(169%)
SAM-10	97.25 \pm 0.04	7820	492(181%)	84.20 \pm 0.08	7820	495(183%)
LookSAM-5	97.23 \pm 0.03	15640	358(132%)	83.23 \pm 0.08	15640	339(125%)
ESAM	97.59 \pm 0.04	\	311(114%)	85.39 \pm 0.09	\	315(116%)
ESAM ¹	<u>97.81\pm0.01</u>	\	401(139%)	85.56 \pm 0.05	\	381(138%)
SAF	97.07 \pm 0.05	\	488(179%)	83.23 \pm 0.06	\	489(180%)
SAF ²	97.34 \pm 0.06	\	391(202%)	84.71 \pm 0.01	\	397(200%)
MESA ²	97.46 \pm 0.09	\	332(171%)	84.73 \pm 0.14	\	339(171%)
AE-SAM ³	97.90\pm0.05	39256	\	85.58 \pm 0.10	38944	\
vSAM	97.49 \pm 0.08	29104	411(151%)	<u>85.67\pm0.06</u>	26972	395(146%)

1 We report the results in [Du *et al.*, 2022a]. But failed to reproduce them using the officially released codes.

2 We report the results in [Du *et al.*, 2022b]. For SAF, we failed to reproduce it using the official released code on CIFAR-10 and CIFAR-100, so we reproduced it ourselves following the algorithmic flow of SAF.

3 We report the results in [Jiang *et al.*, 2023].

Table 3: The results of the proposed method and the comparison methods on CIFAR-10 and CIFAR-100 dataset. The numbers in parentheses (·) indicate the ratio of corresponding method’s training speed to SAM’s. \uparrow means that the larger the reported results are better, and \downarrow means that the smaller the results are better. The best accuracy is in bold and the second best is underlined.

datasets	CIFAR-10		CIFAR-100	
	Acc.	AIS	Acc.	AIS
SAM-5	96.40	2780(156%)	80.42	2763(151%)
vSAM	96.64	2492(140%)	80.76	2470(135%)
vSAM-A	96.60	2405(135%)	80.60	2459(134%)

Table 4: Ablation Study of vSAM on CIFAR-10 and CIFAR-100.

timization speed compared to LookSAM and ESAM. This is because LookSAM involves additional operations, such as computing the gradient projection, while ESAM still requires computing the gradient twice for one optimization step. SAF sacrifices memory for optimization efficiency, achieving nearly the same speed as SGD. MESA accelerates training by utilizing an EMA model and eliminating the need for backward when updating the EMA model. While vSAM may not match the speed of SAF and MESA, it excels in preserving the model’s generalization capability. Furthermore, vSAM achieves comparable performance to AE-SAM with fewer SAM updates.

4.4 Ablation Study

To better understand the effectiveness of adaptive sampling rate and gradient reuse in improving the performance and efficiency, we consider a variant of vSAM: vSAM with only adaptive sampling rate, optimized with SGD during non-sampling iterations (vSAM-A). The results are presented in Table 4.

Compared to SAM-5, optimization speed of vSAM-A is slower because the adaptive sampling rate strategy lets the total sampling number of vSAM-A is larger than SAM-5. However, the accuracy of vSAM-A is higher than that of SAM-5. This indicates that the adaptive sampling rate can effectively enhance optimization speed while preserving the model’s generalization ability. Comparing vSAM with vSAM-A, we observe that the gradient reuse strategy can also prevent the model’s generalization ability without increasing the computational cost.

4.5 Application to Quantization-Aware Training

Neural network quantization reduces computational demands by lowering weight and activation precision, enabling efficient deployment on edge devices without compromising model performance [Esser *et al.*, 2020; Wei *et al.*, 2021; Nagel *et al.*, 2022].

Learned Step size Quantization (LSQ) [Esser *et al.*, 2020] is a commonly used scheme in quantization tasks. The quantization parameter step size is set as a learnable parameter to participate in network training instead of calculating by weight distribution. We employ vSAM as the optimization method for LSQ to demonstrate its broader applicability. We utilized SGD, SAM, and vSAM to quantize the parameters of ResNet-18 and MobileNets to W4A4 on the CIFAR-10 dataset, and the results are presented in Table 5. The training speed of vSAM is over 50% faster than that of SAM, while maintaining results close to SAM. This demonstrates

methods	ResNet-18		MobileNets	
	Acc.	AIS	Acc.	AIS
Full prec.	88.72	\	85.81	\
LSQ+SGD	88.47	1720(191%)	83.44	1740(201%)
LSQ+SAM	89.46	902(100%)	83.83	865(100%)
LSQ+vSAM	89.01	1487(165%)	83.80	1329(154%)

Table 5: Results of optimizing LSQ using vSAM on the Cifar-10 dataset.

that vSAM is versatile and meets the practical requirements for various applications.

5 Conclusions

In this paper, we discover that the gradient of SAM can be decomposed into the gradient of SGD and the PSF. To enhance optimization efficiency, we transform the optimization process of SAM into gradient sampling and gradient reuse of the PSF. We suggest that if the PSF changes slightly, it can be replaced by the previous calculated PSF to reduce the calculation. This allows most optimization iterations to avoid performing two forward and backward, as in the case of SAM. We propose an adaptive and efficient optimization method called vSAM based on the variance and gradient norm values of the PSF. vSAM adaptively adjusts the gradient sampling rate of the PSF to enhance optimization efficiency and reuses the PSF in non-sampling iterations. Experimental results show that vSAM achieves similar generalization performance as SAM and has a faster optimization speed.

References

- [Andriushchenko and Flammarion, 2022] Maksym Andriushchenko and Nicolas Flammarion. Towards understanding sharpness-aware minimization. In *Proceedings of the International Conference on Machine Learning (ICML)*, pages 639–668. PMLR, 2022.
- [Chaudhari *et al.*, 2019] Pratik Chaudhari, Anna Choromanska, Stefano Soatto, Yann LeCun, Carlo Baldassi, Christian Borgs, Jennifer Chayes, Levent Sagun, and Riccardo Zecchina. Entropy-sgd: Biasing gradient descent into wide valleys. *Journal of Statistical Mechanics: Theory and Experiment*, 2019(12):124018, 2019.
- [Chen *et al.*, 2022] Xiangning Chen, Cho-Jui Hsieh, and Boqing Gong. When vision transformers outperform resnets without pre-training or strong data augmentations. 2022.
- [DeVries and Taylor, 2017] Terrance DeVries and Graham W Taylor. Improved regularization of convolutional neural networks with cutout. *arXiv preprint arXiv:1708.04552*, 2017.
- [Dinh *et al.*, 2017] Laurent Dinh, Razvan Pascanu, Samy Bengio, and Yoshua Bengio. Sharp minima can generalize for deep nets. In *Proceedings of the International Conference on Machine Learning (ICML)*, pages 1019–1028. PMLR, 2017.
- [Du *et al.*, 2022a] Jiawei Du, Hanshu Yan, Jiashi Feng, Joey Tianyi Zhou, Liangli Zhen, Rick Siow Mong Goh,

- and Vincent YF Tan. Efficient sharpness-aware minimization for improved training of neural networks. 2022.
- [Du *et al.*, 2022b] Jiawei Du, Daquan Zhou, Jiashi Feng, Vincent Tan, and Joey Tianyi Zhou. Sharpness-aware training for free. *Advances in Neural Information Processing Systems (NeurIPS)*, 35:23439–23451, 2022.
- [Esser *et al.*, 2020] Steven K Esser, Jeffrey L McKinstry, Deepika Bablani, Rathinakumar Appuswamy, and Dharmendra S Modha. Learned step size quantization. In *Proceedings of the International Conference on Learning Representations (ICLR)*, 2020.
- [Foret *et al.*, 2021] Pierre Foret, Ariel Kleiner, Hossein Mobahi, and Behnam Neyshabur. Sharpness-aware minimization for efficiently improving generalization. 2021.
- [Han *et al.*, 2017] Dongyoon Han, Jiwhan Kim, and Junmo Kim. Deep pyramidal residual networks. In *Proceedings of the Conference on Computer Vision and Pattern Recognition (CVPR)*, pages 5927–5935, 2017.
- [He *et al.*, 2016] Kaiming He, Xiangyu Zhang, Shaoqing Ren, and Jian Sun. Deep residual learning for image recognition. In *Proceedings of the Conference on Computer Vision and Pattern Recognition (CVPR)*, pages 770–778, 2016.
- [Hochreiter and Schmidhuber, 1994] Sepp Hochreiter and Jürgen Schmidhuber. Simplifying neural nets by discovering flat minima. *Advances in Neural Information Processing Systems (NeurIPS)*, 7, 1994.
- [Izmailov *et al.*,] Pavel Izmailov, Dmitrii Podoprikin, Timur Garipov, Dmitry Vetrov, and Andrew Gordon Wilson. Averaging weights leads to wider optima and better generalization. pages 876–885.
- [Jiang *et al.*, 2020] Yiding Jiang, Behnam Neyshabur, Hossein Mobahi, Dilip Krishnan, and Samy Bengio. Fantastic generalization measures and where to find them. 2020.
- [Jiang *et al.*, 2023] Weisen Jiang, Hansi Yang, Yu Zhang, and James Kwok. An adaptive policy to employ sharpness-aware minimization. In *Proceedings of the International Conference on Learning Representations (ICLR)*, 2023.
- [Keskar *et al.*, 2017] Nitish Shirish Keskar, Dheevatsa Mudigere, Jorge Nocedal, Mikhail Smelyanskiy, and Ping Tak Peter Tang. On large-batch training for deep learning: Generalization gap and sharp minima. *Proceedings of the International Conference on Learning Representations (ICLR)*, 2017.
- [Krizhevsky *et al.*, 2009] Alex Krizhevsky, Geoffrey Hinton, et al. Learning multiple layers of features from tiny images. 2009.
- [Kwon *et al.*, 2021] Jungmin Kwon, Jeongseop Kim, Hyunseo Park, and In Kwon Choi. Asam: Adaptive sharpness-aware minimization for scale-invariant learning of deep neural networks. In *Proceedings of the International Conference on Machine Learning (ICML)*, pages 5905–5914. PMLR, 2021.
- [Li *et al.*, 2018] Hao Li, Zheng Xu, Gavin Taylor, Christoph Studer, and Tom Goldstein. Visualizing the loss landscape of neural nets. *Advances in Neural Information Processing Systems (NeurIPS)*, pages 6391–6401, 2018.
- [Liu *et al.*, 2020] Chen Liu, Mathieu Salzmann, Tao Lin, Ryota Tomioka, and Sabine Süsstrunk. On the loss landscape of adversarial training: Identifying challenges and how to overcome them. *Advances in Neural Information Processing Systems (NeurIPS)*, 33:21476–21487, 2020.
- [Liu *et al.*, 2022] Yong Liu, Siqi Mai, Xiangning Chen, Choji Hsieh, and Yang You. Towards efficient and scalable sharpness-aware minimization. In *Proceedings of the Conference on Computer Vision and Pattern Recognition (CVPR)*, pages 12360–12370, 2022.
- [Loshchilov and Hutter, 2016] Ilya Loshchilov and Frank Hutter. Sgdr: Stochastic gradient descent with warm restarts. *arXiv preprint arXiv:1608.03983*, 2016.
- [Mulayoff and Michaeli, 2020] Rotem Mulayoff and Tomer Michaeli. Unique properties of flat minima in deep networks. In *Proceedings of the International Conference on Machine Learning (ICML)*, pages 7108–7118. PMLR, 2020.
- [Nagel *et al.*, 2022] Markus Nagel, Marios Fournarakis, Yelysei Bondarenko, and Tijmen Blankevoort. Overcoming oscillations in quantization-aware training. In *Proceedings of the International Conference on Machine Learning (ICML)*, pages 16318–16330. PMLR, 2022.
- [Sun *et al.*, 2021] Xu Sun, Zhiyuan Zhang, Xuancheng Ren, Ruixuan Luo, and Liangyou Li. Exploring the vulnerability of deep neural networks: A study of parameter corruption. In *Proceedings of the AAAI Conference on Artificial Intelligence (AAAI)*, volume 35, pages 11648–11656, 2021.
- [Wei and Ma, 2019] Colin Wei and Tengyu Ma. Improved sample complexities for deep neural networks and robust classification via an all-layer margin. In *Proceedings of the International Conference on Learning Representations (ICLR)*, 2019.
- [Wei *et al.*, 2021] Xiuying Wei, Ruihao Gong, Yuhang Li, Xianglong Liu, and Fengwei Yu. Qdrop: Randomly dropping quantization for extremely low-bit post-training quantization. In *Proceedings of the International Conference on Learning Representations (ICLR)*, 2021.
- [Zagoruyko and Komodakis, 2016] Sergey Zagoruyko and Nikos Komodakis. Wide residual networks. *arXiv preprint arXiv:1605.07146*, 2016.
- [Zhang *et al.*, 2021] Chiyuan Zhang, Samy Bengio, Moritz Hardt, Benjamin Recht, and Oriol Vinyals. Understanding deep learning (still) requires rethinking generalization. *Communications of the ACM*, 64(3):107–115, 2021.
- [Zhang *et al.*, 2023] Xingxuan Zhang, Renzhe Xu, Han Yu, Hao Zou, and Peng Cui. Gradient norm aware minimization seeks first-order flatness and improves generalization. In *Proceedings of the Conference on Computer Vision and Pattern Recognition (CVPR)*, pages 20247–20257, 2023.
- [Zheng *et al.*, 2021] Yaowei Zheng, Richong Zhang, and Yongyi Mao. Regularizing neural networks via adversarial

model perturbation. In *Proceedings of the Conference on Computer Vision and Pattern Recognition (CVPR)*, pages 8156–8165, 2021.

[Zhou *et al.*, 2021] Pan Zhou, Hanshu Yan, Xiaotong Yuan, Jiashi Feng, and Shuicheng Yan. Towards understanding why lookahead generalizes better than sgd and beyond. *Advances in Neural Information Processing Systems (NeurIPS)*, 34:27290–27304, 2021.

[Zhou *et al.*, 2022] Daquan Zhou, Zhiding Yu, Enze Xie, Chaowei Xiao, Animashree Anandkumar, Jiashi Feng, and Jose M Alvarez. Understanding the robustness in vision transformers. In *Proceedings of the International Conference on Machine Learning (ICML)*, pages 27378–27394. PMLR, 2022.

[Zhuang *et al.*, 2022] Juntang Zhuang, Boqing Gong, Liangzhe Yuan, Yin Cui, Hartwig Adam, Nicha Dvornek, Sekhar Tatikonda, James Duncan, and Ting Liu. Surrogate gap minimization improves sharpness-aware training. 2022.